The Cryosphere Discuss., 6, 2399–2436, 2012
www.the-cryosphere-discuss.net/6/2399/2012/
doi:10.5194/tcd-6-2399-2012

The Cryosphere Discussions

The first complete glacier inventory for the whole of Greenland

P. Rastner[1], T. Bolch[1,2], N. Mölg[1], H. Machguth[1,3], and F. Paul[1]

[1]Department of Geography, University of Zurich, Winterthurer Str. 190, 8057 Zurich, Switzerland
[2]Institute for Cartography, Technische Universität Dresden, 01069 Dresden, Germany
[3]Marine Geology and Glaciology, Geological Survey of D. and Gl. – GEUS, Ø. Volgade 10, 1350 København, Denmark

Received: 11 June 2012 – Accepted: 16 June 2012 – Published: 16 July 2012

Correspondence to: P. Rastner (philipp.rastner@geo.uzh.ch)

Published by Copernicus Publications on behalf of the European Geosciences Union.

Abstract

Glacier inventories provide important baseline information for the determination of water resources, glacier-specific changes in area and volume, climate change impacts, and the past, potential and future contribution of glaciers to sea-level rise. Though heavily glacierized and thus highly relevant for all of the above points, such an inventory of all local glaciers and icecaps (GIC) was not available so far for Greenland. Here we present the details and results of our inventory, that has been compiled from more than 70 Landsat scenes mostly acquired between 1999 and 2002 using semi-automated multispectral mapping techniques. A digital elevation model (DEM) was used to derive drainage divides from watershed analysis and topographic parameters for each glacier entity. We assigned to each entity one of three connectivity levels (CL0, CL1, CL2; i.e. no, weak, and strong connection) with the ice sheet to distinguish the local GIC from the ice sheet and its outlet glaciers and to serve the specific needs of different user communities. All GIC larger 0.05 km^2 include ~20 300 entities (of which 900 are marine terminating), covering an area of 129 983±4029 km^2, or 89 273±2767 km^2 without the CL2 GIC. The latter is about 50 % more than according to all previous estimates. Glaciers smaller 0.5 km^2 contribute only 1.5 % to the total area but more than 50 % (11 000) to the total number. In contrast, the 25 largest GIC (>500 km^2) contribute 28 % to the total area, but only 0.1 % to the total number. Most of the ice was located at elevations around 1000 m, except in the eastern sector with elevation arround 1700 m. In addition, a strong dependence of the median elevation to the distance from the ocean was found, but only a weak dependence on aspect. All data will be made available in the Global Land Ice Measurement from Space (GLIMS) glacier database.

1 Introduction

Glaciers and ice caps (GIC in the following) are key indicators of climate change (e.g. Lemke et al., 2007), important water resources, and their melt water could potentially make a substantial contribution to sea-level rise during this century (e.g. Meier et al., 2007; Hock et al., 2009; Radić and Hock, 2010). Related assessments require precise knowledge about their location and extent as available in glacier inventories. The local or peripheral GIC on Greenland are one of the regions with a potentially large contribution to sea-level rise, but also largely absent inventory information (Kargel et al., 2012). Moreover, the situation in Greenland is special due to the highly complex and differently used separation of the ice sheet and its outlet glaciers from the local GIC (Paul, 2011). To overcome this situation and to provide a sound data base for global-scale modelling applications (e.g. Huss and Farinotti, 2012; Radić and Hock, 2010), a complete dataset (vector outlines) of all GIC on Greenland is of high importance.

For the above reasons we have compiled the first glacier inventory of all GIC in Greenland by applying semi-automated glacier-mapping techniques (e.g. Paul and Kääb, 2005) to Landsat imagery in combination with a digital elevation model (DEM) to obtain drainage divides following Bolch et al. (2010) and topographic parameters for each entity following Paul et al. (2009). A rather challenging issue was to define a consistent strategy for separating the GIC from the ice sheet, as the local GIC occur in coastal regions not covered by the ice sheet, and on mountain ridges within the ice sheet (Weidick and Morris, 1998). Considering the varying requirements for the different scientific communities (e.g. sea level change, hydrological, and glaciological modelling), we assigned three connectivity levels (CL) to the local GIC to describe their strength of connection (no, weak, strong) to the ice sheet. This is also, for instance, required to avoid a double counting for their contribution to sea-level rise, as normally used ice-masks for Greenland also include (at least partly) local GIC (Paul, 2011).

So far, only parts of Greenland's GIC were inventoried in detail: the glacier inventory of West Greenland (Weidick et al., 1992), the Geikie glacier inventory (Jiskoot et al., 2012), a glacier inventory of Disko Island and the Nuussuaq and Svartenhuk peninsulas (Citterio et al., 2009). Only two datasets (Geikie plateau and South Kronprins Christian Land) are currently downloadable from the Global Land Ice Measurements from Space (GLIMS) database. Greenland-wide datasets of the ice-covered area (i.e.

without a separation from the ice sheet or drainage divides) that are publicly available exists only from the Digital Chart of the World (DCW) (Danko, 1992) and the outlines from the Greenland Ice Mapping Project (GIMP) provided by Howat and Negrete (2012). A similar comprehensive data set with vector outlines of all GIC and the ice sheet is hold by GEUS (Kargel et al., 2011), but not (yet) available for scientific research. All data sets vary in their degree of generalization, temporal frame, and consideration of details (e.g. debris cover).

Due to the so far missing inventory data (the DCW was never used for that purpose) the total area covered by local GIC on Greenland has been assessed from a range of (not always fully documented) techniques. The reported values range from about 49 000 km^2 (Ohmura, 2009; Weng, 1995) up to 70 000 km^2 (Dyurgerov and Meier, 2005; Weidick and Morris, 1998). Despite this large estimated area (approximately 7 % of all GICs worldwide, cf. Hock et al., 2009), also the calculation of the sea-level rise contribution of Greenland's GIC has so far received only limited attention. The absence of a consistent and complete inventory resulted in the application of either rough extrapolation schemes (Radić and Hock, 2010), their exclusion (Raper and Braithwaite, 2006), or a separate treatment (Lemke et al., 2007).

The main purposes of the here presented new and complete inventory are firstly to close the knowledge gap about the local GIC to improve the estimation of their past, potential and future contribution to global sea-level change for the forthcoming 5th assessment report (AR5) of the IPCC and secondly, to allow proper change assessment. The full data set will be made available in the GLIMS database (Bishop et al., 2004; Raup et al., 2007).

2 Study region and datasets

2.1 Study region

Our study area is entire Greenland (Fig. 1), extending from 60° to 84° N (2650 km) and from 11° to 74° W (1200 km). More than 80 % of Greenland is covered by ice ranging from sea-level to 3200 m a.s.l. along the central dome of the ice sheet and almost to 3700 m a.s.l. on Greenland's highest mountain (Gunnbjørns fjeld). To provide a more regionalized assessment of the GIC characteristics, we divided Greenland in four glaciological sub regions, following the suggestion of Weidick et al. (1995) but adding a further sector in the south.

Greenland's climate is polar to subpolar and acts climatologically as a centre of cooling, and hydrologically as large freshwater storage. Temperatures in Greenland have been monitored since the 1870s showing a distinctive warming trend since the 1980s that increased during the 1990s predominantly on the western coast (Cappelen et al., 2007). The year 2010 was the warmest year across Greenland (except for the north-east) since the start of meteorological observations (Box et al., 2010). The present-day accumulation pattern in Greenland is roughly captured by measurements (Bales et al., 2009; Burgess et al., 2010) and regional climate modelling (Box et al., 2006; Ettema et al., 2009; Fettweis et al., 2008), with large uncertainties remaining in regions where measurements are sparse (Helsen et al., 2012). According to Ohmura and Reeh (1991), the highest annual precipitation amounts occur south of 65° N on the western side (400–1000 mm a^{-1}) and south of 70° on the eastern side (400–2500 mm a^{-1}) of Greenland. The lowest amounts are found in the north-east (100 mm a^{-1}) and locally around Søndre Strømfjord on the western coast and Narssarssuaq in Southern Greenland.

A large variety of glacier types from large ice caps with numerous outlet glaciers, extended valley glaciers, to mountain glaciers of all shapes and small cirques can be found in Greenland. Due to the large south-north extent, different thermal regimes can be expected for the glaciers. Whereas in the north especially cold glaciers are present, in the central part polythermal and in the southern parts also temperate glaciers are found (Bull, 1963; Hammer, 1985). Many glaciers on Greenland have been identified as being of surge type, for instance in the Stauning Alper region (Jiskoot et al., 2001; Weidick, 1988) and in the Disko/Nussuuaq region (Yde and Knudsen, 2005).

2.2 Datasets

We selected 73 of the most suitable (with minimum seasonal snow, and largely cloud free) Landsat scenes available from the glovis.usgs.gov archive, setting a focus on the (undisturbed) Landsat 7 ETM+ scenes (1999–2002). All scenes are listed along with an index map of their footprints in the supplement (Table A1 and Fig. A1). Seasonal snow was a severe problem in the north-eastern part of Greenland and we mosaicked several scanline corrector (SLC) off scenes with much better snow conditions to get an appropriate coverage. We partly also used Landsat TM scenes from the period 1994–2008 to fill local data gaps. It has to be noted that during this period some glaciers have shown considerable changes in extent (e.g. Yde and Knudsen, 2005). The acquisition date of each scene processed is documented in the attribute table of each glacier outline, so that a proper reference for change assessment is available.

To overcome the missing coverage with Landsat data north of 80° N, we used the outlines of the GIMP ice cover map released online http://bprc.osu.edu/GDG/icemask.php (Howat and Negrete, 2012) as baseline information and improved them manually by visual interpretation of a MODIS 250 m image of the same region. This was important as some wrongly classified ice-covered lakes adjacent to outlet glaciers of the Hans Tausen Iskape (cf. Hammer, 1985) and the included ice shelves had to be removed. The GIMP ice cover map does partly not consider debris-covered glaciers and excluded glaciers smaller than 0.05 km^2; in the northern-most region, ice shelves were included as the purpose of that dataset is to include all ice-covered areas.

For this overall inventory we decided to stick to the DEM of the Greenland Mapping Project (GIMP, Howat et al., 2012) with the supplement tile "GI-north" from the website http://viewfinderpanoramas.org (VFP) in the very far north that was not covered by the

GIMP DEM. The GIMP DEM has a resolution of 90 m and a reported vertical accuracy of 10 m. It was merged from several datasets acquired between the years 2000 and 2009. As high-resolution photogrammetric DEM extraction does only provide accurate results in areas with high contrast and does therefore not work well above the snowline, lower spatial resolution DEM data (500 m AVHRR) was merged with the GIMP DEM. The VFP DEMs were mainly created from 1 : 250 000 and 1 : 500 000 scale topographic maps with a locally variable quality (Ferranti, 2012). Additionally, the ASTER GDEM II was used in this study to assess the suitability of the GIMP DEM for extracting topographic parameters in the Stauning Alper region. All place names used here are based on Weidick et al. (1995).

3 Methods

The overall data processing workflow as illustrated in Fig. 2 can roughly be subdivided in three steps: (a) glacier mapping, (b) creation of drainage basins to separate the local GIC from the ice sheet and among each other, and (c) intersection of both datasets with a subsequent calculation of glacier specific statistics. These three steps are described in the following in more detail.

3.1 Glacier mapping

For the glacier mapping we applied the well established semi-automated band ratio method as described by Paul and Kääb (2005). The ratio images were computed from raw digital numbers for Landsat ETM+ bands 3 and 5. An optimal threshold value was chosen for each scene interactively and pixels were classified as glaciers when the band 3/5 ratio > 1.6 to 2.4 (dependent on scene conditions). In the following step a median filter (3×3 kernel) was applied to reduce noise and the classified raster image was converted into a vector format (shapefile). Only glaciers larger than 0.05 km^2 were considered for the inventory and manually corrected where required. The corrections for clouds, shadow, debris cover, seasonal snow and icebergs were time consuming, and took approximately 80 % of the total processing time. Similar to the experience in other regions (e.g. Paul and Andreassen, 2009; Bolch et al., 2010), one of the most challenging questions was related to the correct consideration of extended snow fields that showed no ice but might be perennial rather than seasonal. As a general rule, we included all polygons where exposed ice was visible and excluded most of the "snow only" regions, in particular at low elevations. The correct identification of frozen lakes was in some regions also difficult, a well known problem when working in Arctic regions (e.g. Paul and Kääb, 2005; Racoviteanu et al., 2009). In this study we have additionally used DEM information (hillshades) and multi-temporal satellite images to improve their identification. The mapping and the manual corrections were always performed in the local UTM system (spanning zones 18–28 N). In a second step, the resulting outlines were mosaicked and reprojected to an area-preserving projection (Greenland Lambert Azimuthal Equal Area projection with WGS 1984 datum), as the UTM projection is not area preserving.

The accuracy of the glacier outlines is difficult to assess as appropriate reference data are required but were not available for this region (Andreassen et al., 2008; Paul et al., 2002). However, a recent round robin experiment has analyzed accuracy issues in more detail (Paul et al., 2012) comparing outlines derived automatically and from multiple digitization of the same set of glaciers by the same and different analysts. The study concluded that both methods (manual and automated) have about the same precision for clean ice (standard deviation of 2–5 %) and that debris-covered glacier parts revealed a large variability in interpretation, resulting in area differences higher than 30 %. As the location of the manually digitized outlines varied by about 1 TM pixel or 30 m (for clean ice), we determined the precision of the here-derived outlines by applying a 15 m buffer around all glacier polygons. This gives a 3.1 % larger total area which is in the following used as the measure of uncertainty for the derived area values.

3.2 Drainage divides and assignment of connectivity levels

We derived glacier basins (drainage divides) to separate the ice masses into entities in a two step approach: first, they were automatically calculated in the GIS using watershed analysis following a modified approach developed by Bolch et al. (2010), and in a second step they were manually adjusted using a colour-coded flow direction grid in the background and a set of newly developed rules that are explained in the following.

Firstly, the local GIC were separated from the ice sheet. This was actually rather challenging, as outlet glaciers from otherwise disconnected ice caps can join outlets from the ice sheet (and thus contribute to their flow), or glaciers that are connected to the ice sheet in the accumulation region can have completely separated ablation regions. To also serve the varying requirements of the different modelling communities (e.g. GIC and ice sheets), we decided to define three connectivity levels (CL) of the GIC with the ice sheet:

- CL0: no connection.
- CL1: weak connection (clearly separable by drainage divides in the accumulation region, not connected or only in contact in the ablation region).
- CL2: strong connection (difficult to separate in the accumulation region or joint flow in the ablation region).

To assign the connectivity level automatically in the GIS, we also applied a "topological heritage" rule. Glacier entities connected to other entities that have been assigned CL1 will adopt the same class. This is also the case for entities connected to CL2 entities. CL0 entities (either individual or within a group of connected entities) have no connection to the ice sheet or any of the CL1 or CL2 GIC. A colour-coded illustration of the assigned connectivity levels is depicted in Fig. 3.

Indeed, the topological heritage rule can only be applied after the local GIC were separated into entities. And here the next set of challenges start: as pointed out by

Racoviteanu et al. (2009), separating an ice cap into entities is difficult from a methodological point of view and it can be discussed if an ice cap should be separated into entities at all (glaciological vs. hydrological application). A further tricky issue is that a watershed algorithm can find a very large number of divides (for a near symmetric shape) that do not make sense even from a hydrological point of view. This changes when an ice cap has prominent outlet glaciers and at least some topographic variability (such as the Jostedalsbreen ice cap in Norway). The further set of rules to get the local GIC consistently separated are:

- GIC rule I: divide an ice cap only when it has prominent outlet glaciers and at least some topographic variability in the accumulation area.
- GIC rule II: if one outlet glacier is separated, the entire ice cap has to be divided into entities.
- GIC rule III: for ice caps and glacierized mountain flanks, the smallest number of entities should be assigned, only considering the most prominent topographic divides.

The interpretation of "some topographic variability" is subjective and can be discussed. As an example, we show in Fig. 4 two larger ice caps both having prominent outlet glaciers but only one is separated, as the other one has no topographic variability. The correction of the raw drainage divides provided by the automated watershed algorithm according to the rules above was a tedious and time-consuming work for all local GIC on Greenland. To support interpretation, we additionally used hillshades and contourlines from the DEM as well as contrast enhanced versions of the respective Landsat scenes.

3.3 Topographic parameters and DEM accuracy

Finally, the glacier outlines were digitally intersected with the drainage basins to obtain the glacier entities (cf. Bolch et al., 2010; Paul et al., 2002). This dataset is then digitally combined with the DEM and products thereof to derive a set of topographic parameters (minimum, maximum, mean and median elevation, mean slope and aspect) from zonal statistics (each glacier entity acts as a zone over which the statistics are calculated) following Paul et al. (2009). The smallest glacier in the sample (0.05 km^2) covers only about 6 cells from the GIMP DEM and the quality of the derived parameters can be questioned for such small glaciers. We have thus calculated for a subset of 620 glaciers in the Stauning Alper region (see Fig. 1 for location) the minimum, maximum, mean and median elevation with the GIMP DEM and the ASTER GDEM II. A visual comparison of the hillshades of both DEMs is shown in Fig. 5, highlighting the much more uneven surface (with many artefacts) in the GDEM. We found that the differences of the above parameters between the two DEMs are rather small in the mean (minimum: 67 m, maximum: –46 m, mean: 1 m, and median: 3 m), but the standard deviation of the differences between individual glaciers are rather high (minimum: 636 m, maximum: 609 m, mean: 546 m, and median: 391 m). On that base we decided to use the GIMP DEM throughout.

4 Results

In Fig. 1 we show an overview of all local GIC and their connectivity level. Three large regions, the Pittufik in the north-west, the entire Geikie plateau and the Hutchinson plateau in the east have a CL2 connectivity along with some other regions around Greenland according to our definition. In the southern sector we defined the peninsula in the south-east of “Schweizerland” as CL1, together with three further peninsulas in the far south-east and the Sukkertoppen ice cap. In the northern sector we classified the “North Ice Cap”, the ice cap touching Petermann glacier at the western side, and the ice cap south of J.P. Koch Fjord as CL1. The most prominent examples for the CL1 class in the eastern sector are the two ice caps located at the north and south of Pasterze glacier, the two ice caps south of Wahlenberg Gletscher and the ice cap in the east of Renland (see Fig. 1 for location).

Considering only entities larger than 0.05 km^2, all CL0 and CL1 GIC have a total area of 89 273 ± 2767 km^2. Including also CL2 to the local GIC adds 40 710 ± 1262 km^2 to a total of 129 983 ± 4029 km^2 with ~20 300 GIC overall. The ice sheet itself has an area of ~1 678 500 km^2 according to our dataset and the entire ice covered area in Greenland is thus ~1 800 000 km^2. Hence, the area covered by the local GIC is ~7.2 % of the total ice covered area (Table 1). From the entire sample (including CL2), 907 (4.5 %) GIC are identified as marine terminating with an area of 65 021 ± 2015 km^2 (Table A2). They are mostly found in the south-east and north of Greenland (Fig. A2). The area covered by marine terminating glaciers in the Geikie Plateau is 24 494 km^2 in our study and thus considerably lower than in the study by Jiskoot et al. (2012) who found 41 591 km^2 . This is because in the latter study Christian IV Glacier is included and drainage divides have different positions.

Plotting the area covered and number of glaciers per size class separately for the four sectors, all glaciers and the marine terminating glaciers, reveals interesting differences (Fig. 6). In all sub regions and entire Greenland the size classes 0.1–0.5 and 1.0–5.0 km^2 have the highest relative contributions by number (about 35 and 20 %, respectively), but glaciers <5 km^2 cover only a small part (10 %) of the total area. In contrast, glaciers larger than 10 km^2 contribute only 8 % to the number but nearly 84 % to the total area. This is rather different for the marine terminating glaciers where sizes <5 km^2 contribute 35.6 % to the total number and GIC larger 10 km^2 contribute 64.3 %, i.e. they are much larger in the mean. The mean size of the GIC per sector (east, north, south and west) is 7.2, 12.8, 3.3 and 2.2 km^2 and 6.4 km^2 for all GIC, whereas it is 71.6 km^2 for the marine terminating glaciers. In absolute terms, the largest glaciers are found in the east and north (Fig. 5; Table A3) followed by the south and west. The second largest glacier class (50–500 km^2) is dominant in the north where large ice caps are present. The small glaciers are mostly found in the southern and eastern sector.

The analysis of the area distribution per aspect sector for all glaciers (CL0 and CL1 only) revealed a clustering towards N and SW for the northern sector and NW to SE for the southern sector (Fig. 7a). The GIC in the eastern and western sector show a rather uniform aspect distribution. This is also the case for entire Greenland (with a small preference for N and SW aspects). The absolute area covered per aspect sector is listed in Table A4.

The area-elevation distributions for each main sector and all of Greenland is depicted in Fig. 7b for the classes CL0 and CL1 and for all classes separately. The largest ice-covered areas can be found in the north and east sectors with a remarkably different maximum around 1000 m a.s.l. and 1700 m a.s.l., respectively. The much lower peak elevation in the northern sector can be ascribed to the topography (ice caps with a peak elevation) and maybe also to the lower mean annual air temperature (MAAT) in this region. The special topography of the numerous ice caps also create a sharp drop in the ice-covered area below 1000 m. In contrast, the west and south sector contain much less ice and its distribution with elevation is more homogenous. Peak values are found at 900 and 1200 m a.s.l. The lower elevation in the southern sector hints to a very reduced influenced of the MAAT. The CL2 glaciers increase the area covered for the eastern sector considerably, but the overall distribution is rather similar. Above 2000 m a.s.l. ice is only found in the eastern sector and is thus the same as for entire Greenland. Taken together, the peak elevation is around 1000 m a.s.l. either with CL2 GIC or without them.

In Fig. 8 the spatial distribution of median elevation is shown as colour-coded circles for all GIC larger than 0.1 km^2. A strong gradient from the coast to the interior can be seen all around Greenland with lowest values closest to the coast (0–400 m) and increasingly higher values (up to 2400 m) towards the interior. When interpreting the median elevation as a proxy for the equilibrium line altitude (ELA) and hence as an indicator of the precipitation regime of a region (e.g. Braithwaite and Raper, 2009), a decreasing precipitation trend from the coast to the interior of Greenland can be derived.

5 Discussion

5.1 Assignment of connectivity levels

The assignment of connectivity levels and the rules to separate ice caps into entities are certainly a matter of discussion. Already Weidick et al. (1992) mentioned the separation of the local GIC from the ice sheet as a major problem for Greenland. The GIC CL2 was introduced to retain strongly connected local GIC with the ice sheet, as the ice sheet modellers wanted to have them as a part of the ice sheet, but the GIC modellers not. So the hydrologic divides as derived from watershed analysis are fine by themselves, but need human interpretation to serve various communities. The interpretation provided here is seen as a starting point to solve the issue, as for example the precise calculation of the past or future sea level contribution of the GIC is also strongly dependent on the divides to avoid a double counting in related assessments (Paul, 2011). When better suggestions for a consistent separation come up, it should be possible to refine the divides as all datasets are digitally available. The manual correction of the drainage divides was time consuming, but clearly faster than the manual correction of the glacier mapping errors (debris, shadow, seasonal snow). According to our rules, the Julianehåb and Inglefield ice doms have been interpreted as being part of the ice sheet in our inventory. Weidick et al. (1992), however, counted these ice masses as being local, but this is not compliant with the extent used in current ice sheet models (e.g. Fettweis et al., 2008), so we have decided to exclude them from the local GIC.

5.2 Comparison to other datasets

The comparison in Table 2 of all glaciers >0.05 km^2 with CL0 connectivity to the other two available Greenland-wide datasets (DCW, GIMP) reveals that the area is highest in our dataset (65 150 ± 2019 km^2), second highest in the GIMP dataset (61 610 km^2) and lowest in the DCW dataset (57 715 km^2). This indicates that the generalization in the DCW and the missing debris cover in the GIMP outlines make quite a difference (−11 % and −5 %, respectively) for the total area covered. The glacier outlines from the hydrologic layer of the DCW are based on digitized 1 : 1 000 000 scale topographic maps and are thus expected not to include most of the smaller glaciers.

Earlier studies used a wide range of techniques to estimate the total area covered by local GIC (for a detailed description see Cogley, 2012). The values range from about 49 000 km^2 (Ohmura, 2010; Weng, 1995), over 54 400 km^2 (Radić and Hock, 2010) up to 70 000 km^2 (Dyurgerov and Meier, 2005; Weidick and Morris, 1998). The values derived here (~89 273 ± 2767 km^2 for CL0 and CL1, ~129 983 ± 4029 km^2 incl. CL2) are thus about 50 % and 100 % larger than the mean value of the previous estimates. It has to be noted that Weidick and Morris (1998) also include CL2 GIC in their estimate as well as some larger ice domes (e.g. Julianehab) that are not included in our assessment. The much higher total area found here implies that also the volume from the local GIC (and hence their potential sea-level rise contribution) is higher than assumed in previous studies.

5.3 Inventory data

The distribution of the area and number of glaciers per size class is similar to other regions in the world and should allow to obtain the total area covered by upscaling the size class distribution. However, some regional variability exist and the sample used in the study by Radić and Hock (2010) was likely not too representative for other regions. The presented total number of GIC (20 300) should be seen as a rough estimate that changes with the rules applied for creating drainage divides. The latter also determine (along with the topography in each sector) the here presented aspect distribution. Although the mean aspect for ice caps is rather arbitrary (also when divided into entities), a certain preference might be found in regions with other glacier types (Evans, 2006). We found no dependence of mean or median elevation on aspect, but an increase of median elevation with distance from the ocean. This hints to a decrease of precipitation amounts from the coast to the interior of Greenland. Such a trend was also found in other studies (Le Bris et al., 2011; Paul et al, 2011), and is confirmed here for the first time from the topographic glacier parameters in Greenland. To derive such a trend from measurements is difficult, because on Greenland weather stations are either coastal (Danish Meteological Institute stations) or are located on the ice sheet (GC-Net and PROMICE Network, Ahlstrøm et al., 2008; Steffen and Box, 2001). Furthermore, weather stations from the latter two networks do only measure accumulation but not precipitation.

5.4 DEM impacts

The quality of the new inventory also depends on the quality of the DEM applied. On one hand, the DEM should have a high resolution and be compiled around the year 2000 (close to the acquisition date of the satellite images used to derive the outlines) and on the other hand it should be precise and have no artefacts. The GIMP (and VFP) DEM used here provide both drainage divides and topographic parameters. Applying another DEM will result in different drainage divides (location and number) as well as different topographic parameters. However, the comparison with the GDEM II clearly revealed that the GIMP DEM is preferable for both, mostly due to the many artefacts still present in the GDEM. So before a new and more precise DEM is released (e.g. from the TanDEM-X mission), the values calculated here have likely the highest quality possible today.

5.5 Accuracy

Apart from the methodological constraints (position of ice divides, interpretation of perennial snow fields), we assume that the accuracy of the glacier outlines is similar to other studies that have applied automated mapping in combination with manual correction. With the buffer method we derived an area uncertainty of about 3 % in the mean over all glaciers; indeed this value can be much higher for individual glaciers and those with debris cover. Of course, towards smaller glaciers the relative area uncertainty also increases. Though the mapping of ice caps is straight forward due to the generally missing debris cover, attached snow patches (either seasonal or perennial) introduced considerably uncertainty in particular in the northern sector. Debris-covered tongues could mostly be delineated precisely as low solar elevation provides sufficient illumination differences. However, for small glaciers and those located in regions of permafrost, the issue is more challenging. But this is again more an interpretation issue rather than an accuracy issue (Citterio et al., 2010).

The impact of the missing glacier area in SLC-off scenes from Landsat ETM+ are locally non-negligible, but overall smaller than other uncertainties. Without using these scenes, especially in the northern sector, it would have been nearly impossible to determine whether some mapped features were glaciers or local snow patches. In this regard, the mosaicing of several SLC-off scenes with much better snow conditions than available from the normal scenes was worth the effort.

6 Conclusions

We presented the first satellite-derived glacier inventory for entire Greenland based on multispectral classification and manual editing of more than 70 Landsat scenes that were available from http://glovis.usgs.gov. Additionally, we included data from an ice-cover map (available from http://bprc.osu.edu/GDG/icemask.php) for the northernmost part of Greenland that is not covered by Landsat. The new inventory revealed a 50 % higher total area (89 273 ± 2767 km^2) than previously assumed. Considering also glaciers with a strong connectivity to the ice sheet (CL2) as being local, yields a total area of 129 983 ± 4029 km^2 and ~20 300 entities (of which about 900 were marine terminating with an area of 65 021 ± 2015 km^2). This much higher area indicates the importance of assigning connectivity levels to each entity to separate the sample according to the needs of different user communities. While this assignment could be implemented more or less automatically, the separation of the local GIC into entities was tedious and time consuming work and might not yet be fully consistent. The location of drainage divides depends on the DEM used and the rules applied to separate entities, differences to other assessments can thus be expected. However, as all data will be available in digital form in the GLIMS database, they can be adjusted and improved once more appropriate input datasets become available.

The correction of the automatically mapped glacier outlines (e.g. for debris, shadow and snow) took about 80 % of the glacier mapping effort. Glaciers smaller 0.05 km^2 were excluded to reduce the impact of seasonal snow. We applied a 1/2 pixel buffer around all outlines and determined a digitizing precision of 3 % (in the mean for all glaciers). The obtained size-class distribution by number and area is similar to other regions in the world and the highest (lowest) number of local GIC is found in the east (west) sector, largely due to the different topographic conditions in both regions. We found a dependence of glacier aspect only in the north and south sector, whereas the other sectors show a uniform distribution. The dependence of median elevation on the distance from the ocean hints to strongly decreasing precipitation amounts from the coast to the interior of Greenland. Most of the glacier area is located around 1700 m a.s.l. in the east sector, and around 1000 m a.s.l. in all other sectors. In view of current approaches to determine the future evolution of GIC under various scenarios of climate change, we recommend to use the CL0 and CL1 GIC as derived here in combination with the GIMP DEM.

Acknowledgement. This work was supported by the ESA project Glaciers_cci (4000101778/10/I-AM) and funding from the ice2sea programme from the European Union 7th Framework Programme, grant number 226375. Ice2sea contribution number 097. Landsat scenes were obtained from USGS (http://glovis.usgs.gov/), and MODIS scenes from the NASA-Reverb website (http://reverb.echo.nasa.gov/reverb/). Glacier outlines in the north of Greenland were downloaded from the Ohio State University – Byrd Polar Research Center webpage (http://bprc.osu.edu/GDG/icemask.php). We gratefully acknowledge Le Bris Raymond for his help with the digitizing and Ian Howat (Ohio State University) for providing us the GIMP DEM.

References

Ahlstrøm, A. P., Gravesen, P., Bech Andersen, S., van As, D., Citterio, M., Fausto, R. S., Nielsen, S., Jepsen, H. F., Kristensen, S. S., Christensen, E. L., Stenseng, L., Forsberg, R., Hanson, S., and Petersen, D.: A new programme for monitoring the mass loss of the Greenland ice sheet, Geol. Surv. Denmark Greenland Bull., 15, 61–64, 2008.

Andreassen, L. M., Paul, F., Kääb, A., and Hausberg, J. E.: Landsat-derived glacier inventory for Jotunheimen, Norway, and deduced glacier changes since the 1930s, The Cryosphere, 2, 131–145, doi:10.5194/tc-2-131-2008, 2008.

Bales, R. C., Guo, Q., Shen, D., McConnell, J. R., Du, G., Burkhart, J. F., Spikes, V. B., Hanna, E., and Cappelen, J.: Annual accumulation for Greenland updated using ice core data developed during 2000–2006 and analysis of daily coastal meteorological data, J. Geophys. Res, 114, D06116, 2009.

Bishop, M. P., Olsenholler, J. A., Shroder, J. F., Barry, R. G., Raup, B. H., Bush, A. B. G., Copland, L., Dwyer, J. L., Fountain, A. G., Haeberli, W., Kääb, A., Paul, F., Hall, D. K., Kargel, J. S., Molnia, B. F., Trabant, D. C., and Wessels, R.: Global Land Ice Measurements from Space (GLIMS): remote sensing and GIS investigations of the Earth's cryosphere, Geocarto Int., 19, 57–84, 2004.

Bolch, T., Menounos, B., and Wheate, R.: Landsat-based inventory of glaciers in Western Canada, 1985–2005, Remote Sens. Environ., 114, 127–137, 2010.

Box, J. E., Bromwich, D. H., Veenhuis, B. A., Bai, L. S., Stroeve, J. C., Rogers, J. C., Steffen, K., Haran, T., and Wang, S. H.: Greenland ice sheet surface mass balance variability (1988–2004) from calibrated polar MM5 output, J. Climate, 19, 2783–2800, 2006.

Braithwaite, R. J. and Raper, S. C. B.: Estimating equilibrium-line altitude (ELA) from glacier inventory data, Ann. Glaciol., 50, 127–132, 2009.

Bull, C. and Studies, O. S. U. I. P.: Glaciological reconnaissance of the Sukkertoppen ice cap, South-West Greenland, Ohio State University, Institute of Polar Studies, Columbus, 1963.

Burgess, E. W., Forster, R. R., Box, J. E., Mosley-Thompson, E., Bromwich, D. H., Bales, R. C., and Smith, L. C.: A spatially calibrated model of annual accumulation rate on the Greenland ice sheet (1958–2007), J. Geophys. Res., 115, F02004, 2010.

Cappelen, J., Laursen, E. V., Jørgensen, P. V., and Kern-Hansen, C.: DMI monthly Climate Data Collection 1768–2006, Denmark, The Faroe Islands and Greenland, Technical Report 07-06, 2007.

Citterio, M., Paul, F., Ahlstrom, A. P., Jepsen, H. F., and Weidick, A.: Remote sensing of glacier change in West Greenland: accounting for the occurrence of surge-type glaciers, Ann. Glaciol., 50, 70–80, 2010.

Danko, D. M.: The digital chart of the world project, Photogramm. Engin. Remote Sens., 58, 1125–1128, 1992.

Dyurgerov, M. B. and Meier, M. F.: Glaciers and the Changing Earth System: a 2004 Snapshot, Institute of Arctic and Alpine Research, Occasional Paper, p. 58, 2005.

Ettema, J., Van Den Broeke, M. R., Van Meijgaard, E., Van De Berg, W. J., Bamber, J. L., Box, J. E., and Bales, R. C.: Higher surface mass balance of the Greenland ice sheet revealed by high-resolution climate modeling, Geophys. Res. Lett., 36, 1–5, 2009.

Fettweis, X., Hanna, E., Gallée, H., Huybrechts, P., and Erpicum, M.: Estimation of the Greenland ice sheet surface mass balance for the 20th and 21st centuries, The Cryosphere, 2, 117–129, doi:10.5194/tc-2-117-2008, 2008.

Hammer, C. U.: The Hans Tausen Ice Cap, Meddelelser om Grønland, Geoscience, 39, 1–165, 2001.

Helsen, M. M., van de Wal, R. S. W., van den Broeke, M. R., van de Berg, W. J., and Oerlemans, J.: Coupling of climate models and ice sheet models by surface mass balance gradients: application to the Greenland Ice Sheet, The Cryosphere, 6, 255–272, doi:10.5194/tc-6-255-2012, 2012.

Hock, R., de Woul, M., Radic, V., and Dyurgerov, M.: Mountain glaciers and ice caps around Antarctica make a large sea-level rise contribution, Geophys. Res. Lett., 36, L07501, 2009.

Howat, I. and Negrete, A.: A high-resolution ice mask for the Greenland Ice Sheet and peripheral glaciers and icecaps, in preparation, 2012.

Howat, I., Negrete, A., Scambos, T., and Haran, T.: A high-resolution elevation model for the Greenland Ice Sheet from combined stereoscopic and photoclinometric data, in preparation, 2012.

Huss, M. and Farinotti, D.: A new approach for estimating ice thickness distribution of 90 000 mountain glaciers around the globe, 14 (EGU2012-4697, 2012), EGU General Assembly, Vienna, 2012.

Jiskoot, H., Pedersen, A. K., and Murray, T.: Multi-model photogrammetric analysis of the 1990s surge of Sortebræ, East Greenland, J. Glaciol., 47, 677–687, 2001.

Jiskoot, H., Juhlin, D., St. Pierre, H., and Citterio, M.: Tidewater glacier fluctuations in central East Greenland coastal and fjord regions (1980s–2005), Ann. Glaciol., 53, 35–44, doi:10.3189/2012AoG60A030, 2012.

Kargel, J. S., Ahlstrøm, A. P., Alley, R. B., Bamber, J. L., Benham, T. J., Box, J. E., Chen, C., Christoffersen, P., Citterio, M., Cogley, J. G., Jiskoot, H., Leonard, G. J., Morin, P., Scambos, T., Sheldon, T., and Willis, I.: Brief communication Greenland's shrinking ice cover: "fast times" but not that fast, The Cryosphere, 6, 533–537, doi:10.5194/tc-6-533-2012, 2012.

Le Bris, R., Paul, F., Frey, H., and Bolch, T.: A new satellite-derived glacier inventory for Western Alaska, Ann. Glaciol., 52, 135–143, 2011.

Lemke, P.: Climate change 2007: the physical science basis: contribution of Working Group I to the Fourth Assessment Report of the Intergovernmental Panel on Climate Change, Cambridge University Press, Cambridge, 2007.

Meier, M. F., Dyurgerov, M. B., Rick, U. K., O'Neel, S., Pfeffer, W. T., Anderson, R. S., Anderson, S. P., and Glazovsky, A. F.: Glaciers dominate eustatic sea-level rise in the 21st century, Science, 317, 1064–1067, doi:10.1126/science.1143906, 2007.

Ohmura, A.: Completing the world glacier inventory, Ann. Glaciol., 50, 144–148, 2010.

Ohmura, A. and Reeh, N.: New precipitation and accumulation maps for Greenland, J. Glaciol, 37, 140–148, 1991.

Paul, F.: Melting glaciers and ice caps, Nat. Geosci., 4, 71–72, 2011.

Paul, F. and Andreassen, L. M.: A new glacier inventory for the Svartisen region, Norway, from Landsat ETM+ data: challenges and change assessment, J. Glaciol., 55, 607–618, 2009.

Paul, F. and Kaab, A.: Perspectives on the production of a glacier inventory from multispectral satellite data in Arctic Canada: Cumberland Peninsula, Baffin Island, Ann. Glaciol., 42, 59–66, 2005.

Paul, F., Kaab, A., Maisch, M., Kellenberger, T., and Haeberli, W.: The new remote-sensing-derived Swiss glacier inventory: I. Methods, Ann. Glaciol., 34, 355–361, 2002.

Paul, F., Barry, R. G., Cogley, J. G., Frey, H., Haeberli, W., Ohmura, A., Ommanney, C. S. L., Raup, B., Rivera, A., and Zemp, M.: Recommendations for the compilation of glacier inventory data from digital sources, Ann. Glaciol., 50, 119–126, 2009.

Paul, F., Barrand, N., Berthier, E., Bolch, T., Casey, K., Frey, H., Joshi, S. P., Konovalov, V., Le Bris, R., Mölg, N., Nosenko, G., Nuth, C., Pope, A., Racoviteanu, A., Rastner, P., Raup, B., Scharrer, K., Steffen, S., and Winsvold, S.: On the accuracy of glacier outlines derived from remote sensing data, submitted to Ann. Glaciol., 54, 2012.

Radić, V. and Hock, R.: Regional and global volumes of glaciers derived from statistical upscaling of glacier inventory data, J. Geophys. Res, 115, F01010, 2010.

Raper, S. C. and Braithwaite, R. J.: Low sea level rise projections from mountain glaciers and icecaps under global warming, Nature, 439, 311–313, 2006.

Raup, B., Kääb, A., Kargel, J. S., Bishop, M. P., Hamilton, G., Lee, E., Paul, F., Rau, F., Soltesz, D., Khalsa, S. J., Beedle, M., and Helm, C.: Remote sensing and GIS technology in the Global Land Ice Measurements from Space (GLIMS) project, Comput. Geosci., 33, 104–125, 2007.

Steffen, K. and Box, J. E.: Surface climatology of the Greenland ice sheet: Greenland Climate Network 1995–1999, J. Geophys. Res., 106, 951–964, 2001.

Weidick, A.: Surging glaciers in Greenland – a status, Rapp. Grønl. Geol. Unders., 140, 106–110, 1988.

Weidick, A. and Morris, E.: Local glaciers surrounding the continental ice sheets, in: Into the Second Century of World Glacier Monitoring – Prospects and Strategies, edited by: W. Haeberli, M. Hoelzle, and S. Suter, A contribution to the IHP and the GEMS. Prepared by the World Glacier Monitoring Service UNESCO, Chapt. 12, 197–207, 1998.

Weidick, A., Boeggild, C. E., and Knudsen, N. T.: Glacier inventory and atlas of West Greenland, Rapp. Grønl. Geol. Unders., 158, 1992.

Weidick, A., Williams, R. S., and Ferrigno, J. G.: Satellite Image Atlas of Glaciers of the World: Greenland, US Government Printing Office, 1995.

Weng, W. L.: The area of Greenland and the ice cap. Letter to the editor, Arctic, 48, 206–206, 1995.

Yde, J. C. and Knudsen, N. T.: Observations of debris-rich naled associated with a major glacier surge event, Disko Island, West Greenland, Permafrost Periglac. Process., 16, 319–325, doi:10.1002/ppp.533, 2005.

Table 1. Area coverage and number per connectivity level.

	Area (km^2)			
	CL0	CL1	CL2	
GIC	65 146 ± 2019	24 127 ± 747	40 710 ± 1262	
Ice sheet	1 743 335	1 784 353	1 767 773	
Total	1 808 480	1 808 480	1 808 480	
	Number			
	CL0	CL1	CL2	Total
GIC	16 655	1771	1855	20 281

Table 2. Available vector data sets of the local GIC on Greenland and how they differ. The "area covered (GIC)" row referes to connectivity levels CL0 and CL1. The GGI (Greenland Glacier Inventory) dataset includes the improved GIMP dataset (covering 14 068 km^2) in the northern-most part of Greenland.

	DCW	GIMP	GGI
Source	Maps 1:1 000 000	Optical/radar	Landsat + GIMP
Period	1950s–1980s	1999–2001	1999–2004
Generalization	High	None	None
Drainage divides	No	No	Yes
Spatial resolution	approx. 2 km	15 m	30 m
Smallest unit mapped	0.1 km^2	0.05 km^2	0.05 km^2
Debris cover included?	Yes	No	Yes
Northern-most region?	Yes	Yes	Yes (GIMP data)
Availability	Free	Free	Free
Area covered (LGIC with CL0 connectivity)	57 715 km^2	61 610 km^2	65 146 ± 2019 km^2
Area covered (total)	1 825 030 km^2	1 798 960 km^2	1 808 480 km^2
Percentage	100.9	99.5	100.0

Table A1. Overview of the Landsat scenes used in this study. The numbers in the column "Label" refer to Fig. A1.

Label	Path	Row	Date	Label	Path	Row	Date
0	228	9	19.08.2000	36	231	14	07.09.1999
1	35	3	24.07.1999	37	5	16	25.08.2000
2	33	1	26.06.2000	38	21	1	01.01.2004
3	31	5	28.06.2000	39	12	2	23.07.2005
4	29	6	23.08.2002	40	12	10	16.08.2002
5	18	8	07.08.2001	41	229	11	12.07.2001
6	23	6	26.08.2001	42	3	17	27.08.2000
7	39	1	20.07.1999	43	19	1	01.01.2004
8	39	2	20.07.1999	44	10	2	20.07.2003
9	19	7	30.08.2001	45	10	11	15.08.2001
10	35	4	24.07.1999	46	227	11	28.08.2000
11	26	6	27.07.2000	47	1	5	01.07.2004
12	13	1	03.07.2001	48	8	3	01.07.2008
13	230	7	20.08.2001	49	8	12	01.08.2001
14	230	8	20.08.2001	50	24	1	01.01.2004
15	230	9	20.08.2001	51	225	11	05.09.2002
16	230	10	21.09.2001	52	15	1	01.07.2003
17	4	5	26.07.2003	53	15	9	21.08.2002
18	20	1	01.01.2004	54	232	6	01.01.2004
19	228	12	11.08.1999	55	6	15	31.07.2009
20	2	17	23.08.2001	56	22	1	01.01.2004
21	226	12	08.08.2001	57	231	11	09.09.2000
22	16	1	01.07.2003	58	232	8	18.08.2001
23	233	14	27.07.2002	59	224	10	14.09.2002
24	233	15	27.07.2002	60	228	10	19.08.2000
25	233	16	10.09.2001	61	9	13	12.07.1994
26	233	17	12.08.2002	62	8	13	01.08.2001
27	233	18	12.08.2002	63	8	14	14.08.2000
28	7	3	01.07.2003	64	45	1	30.06.2000
29	7	4	31.07.2003	65	27	1	02.06.2006
30	7	13	23.08.2000	66	228	10	06.08.2001
31	7	14	23.08.2000	67	12	11	29.08.2001
32	23	1	01.01.2004	68	35	1	24.06.2000
33	231	6	07.09.2005	69	35	5	06.07.2010
34	231	12	14.08.2002	70	227	11	28.08.2000
35	231	13	09.09.2000	71	40	1	03.07.2002
				72	226	10	14.08.2003

Table A2. Number and area of marine terminating glaciers per sector for all connectivity levels.

	Number	Area (km^2)
East	379	31 952
North	214	20 579
South	296	12 146
West	18	344
Total	907	65 021 ± 2015 km^2

Title Page
Abstract | Introduction
Conclusions | References
Tables | Figures
◀◀ | ▶▶
◀ | ▶
Back | Close
Full Screen / Esc
Printer-friendly Version
Interactive Discussion

Table A3. Absolute numbers for Fig. 6 for all connectivity levels per sector, entire Greenland and the marine terminating glaciers.

	North		South		East	
	Number	Area (km^2)	Number	Area (km^2)	Number	Area (km^2)
0.05–0.1	372	25	1530	108	970	69
0.1–0.5	1230	274	2471	566	3069	722
0.5–1.0	320	227	668	473	1042	742
1.0–5.0	687	1715	1050	2333	1832	4262
5.0–10.0	274	1951	208	1485	448	3108
10.0–50.0	423	9643	193	4127	504	10 567
50.0–500.0	167	20 973	76	9257	129	14 595
>500	5	9849	4	2658	15	24 293
Total	3478	44 661	6200	21 011	8009	58 363

	West		Entire GL		Marine term. GIC	
	Number	Area (km^2)	Number	Area (km^2)	Number	Area (km^2)
0.05–0.1	483	34	3355	238	5	0.2
0.1–0.5	917	222	7687	1787	70	24
0.5–1.0	351	252	2381	1696	56	46
1.0–5.0	549	1268	4118	9583	192	498
5.0–10.0	158	1101	1088	7641	122	886
10.0–50.0	128	2478	1248	26 817	287	6755
50.0–500.0	7	455	379	45 282	154	21 731
>500	1	135	25	36 936	21	35 081
Total	2594	5948	20 281	129 983	907	65 021

Table A4. Total area in km^2 for Fig. 7a per sector and entire Greenland (CL0, CL1).

	North	West	East	South	Entire GL
N	10 063	205	4578	590	15 437
NE	5149	598	4080	1995	11 824
E	1080	1076	4665	866	7689
SE	1611	482	2373	3096	7564
S	5119	1042	3894	966	11 023
SW	11 413	819	2113	772	15 118
W	3973	467	3120	1673	9235
NW	3898	987	832	5664	11 383
Total	42 310	5693	25 659	15 623	89 273

Title Page
Abstract | Introduction
Conclusions | References
Tables | Figures
◀| |▶
◀ ▶
Back | Close
Full Screen / Esc
Printer-friendly Version
Interactive Discussion

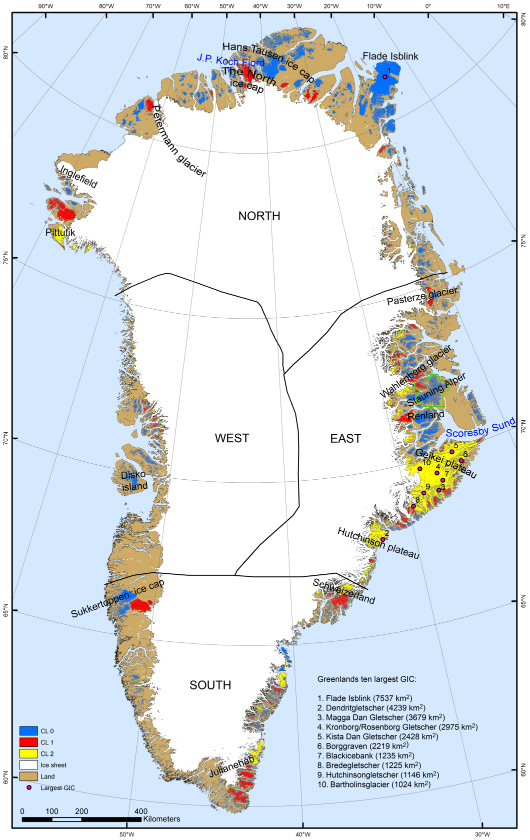

Fig. 1. Map of Greenland showing all local GIC (colour coded) and place names mentioned in the text. The separation of four sub-regions is shown by black solid lines. Local GIC are coloured according to connectivity level to the ice sheet: blue (CL0), red (CL1) and yellow (CL2). The green box indicates the area selected for the investigation of DEMs.

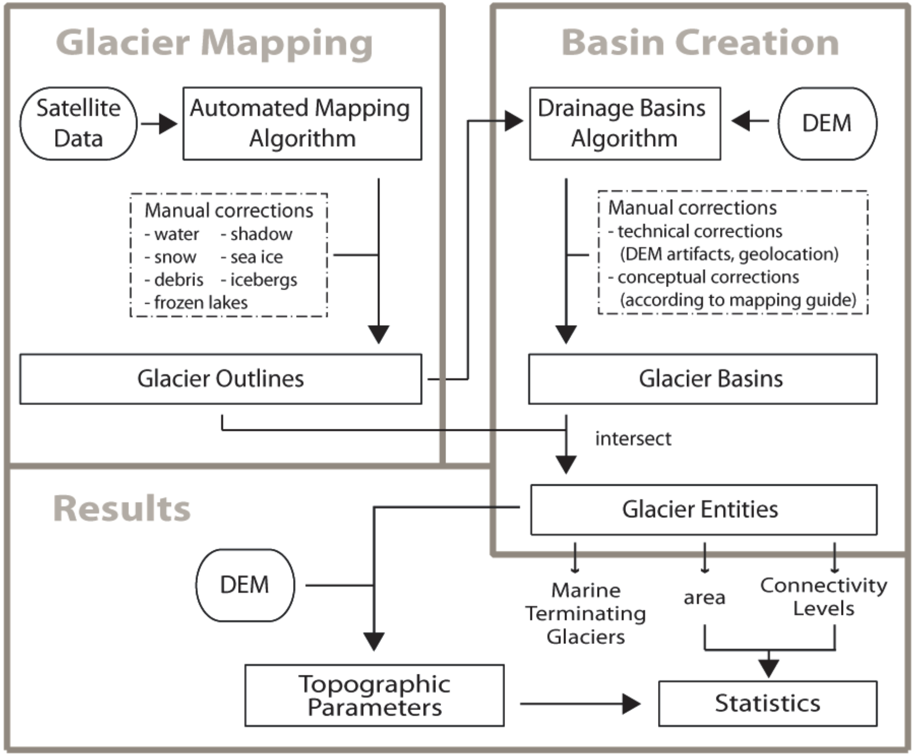

Fig. 2. Flow chart illustrating how the individual processing steps are connected.

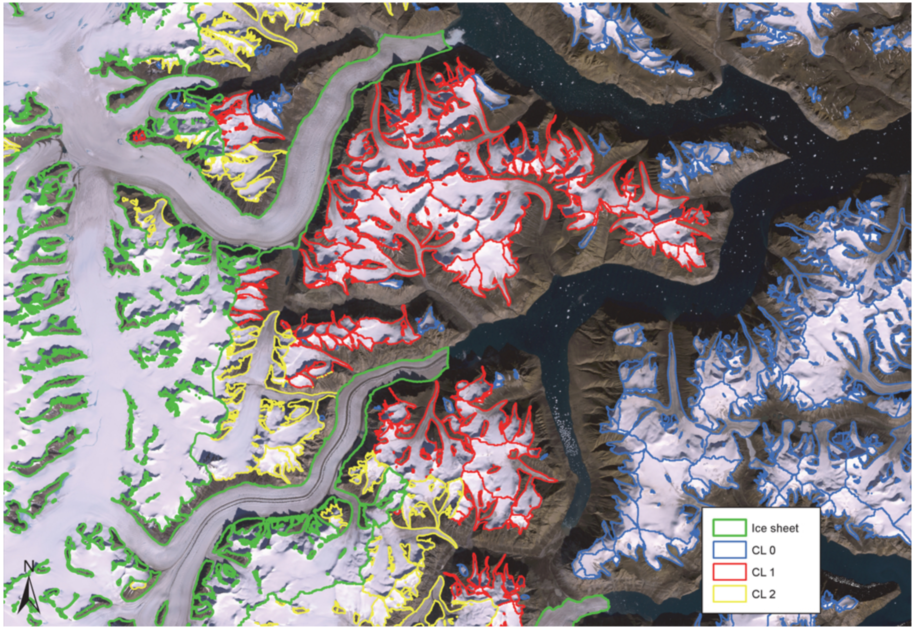

Fig. 3. Close-up of the assigned connectivity levels (colour-coded). As long as glaciers are connected, they have the same connectivity as their neighbours.

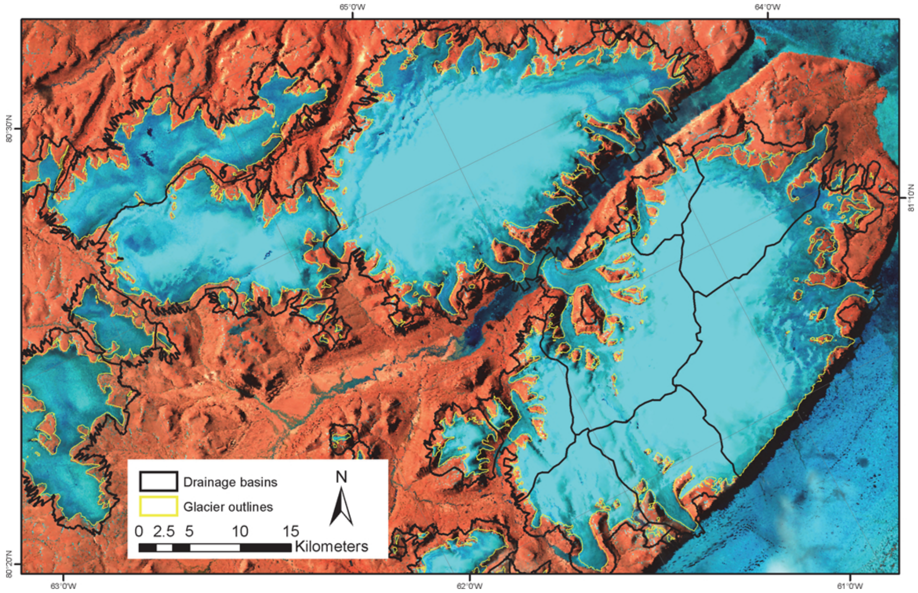

Fig. 4. Separation of ice caps into glacier entities and from each other. Though the large ice cap in the upper centre has several distinct outlet glaciers, it is not separated, as topographic structure is missing in the accumulation area.

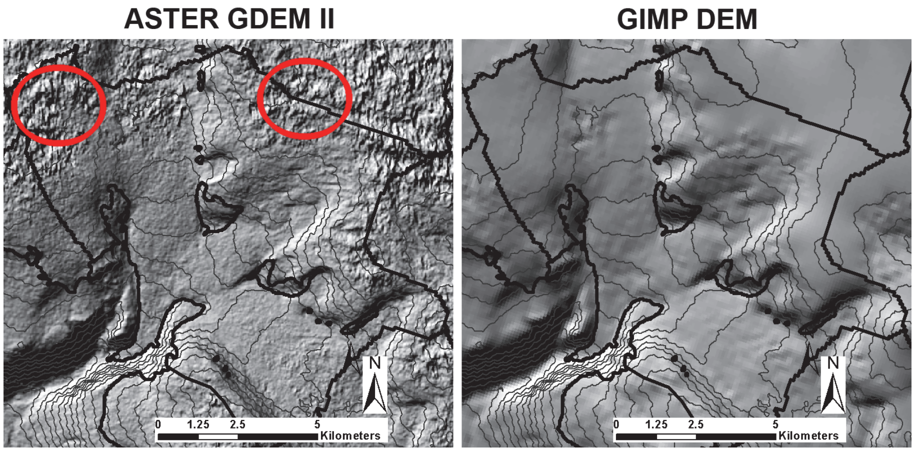

Fig. 5. Comparison of hillshades derived from the GIMP DEM and the ASTER GDEM II for a small subregion in the test area. Red circles indicate artefacts in the ASTER GDEM II due to low contrast at high elevations.

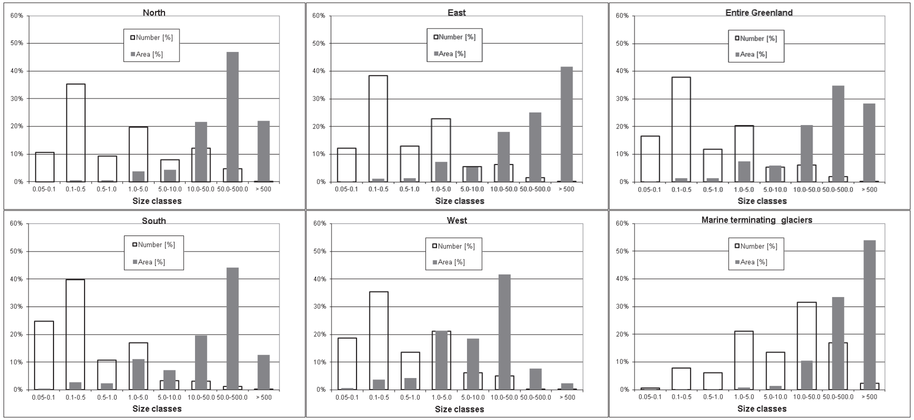

Fig. 6. Number of glaciers and area covered per size class and for each sector, entire Greenland and the marine terminating glaciers.

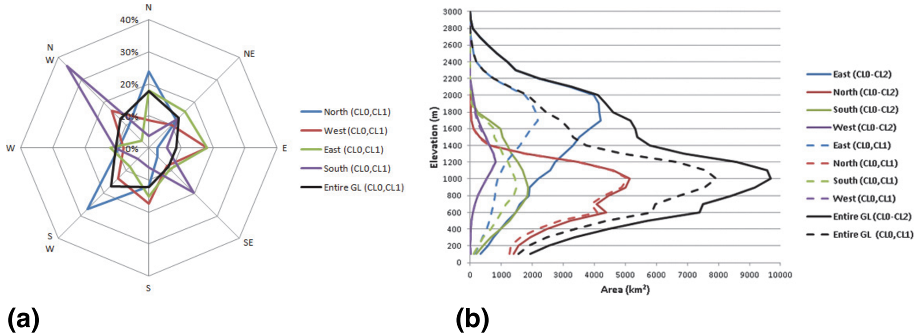

Fig. 7. (a) Area distribution versus aspect per sector for all GIC with CL0 and CL1. **(b)** Area-elevation distribution in 100 m bins for the four sectors and all of Greenland. Dotted lines show the hypsometry for GIC with CL0 and CL1 only.

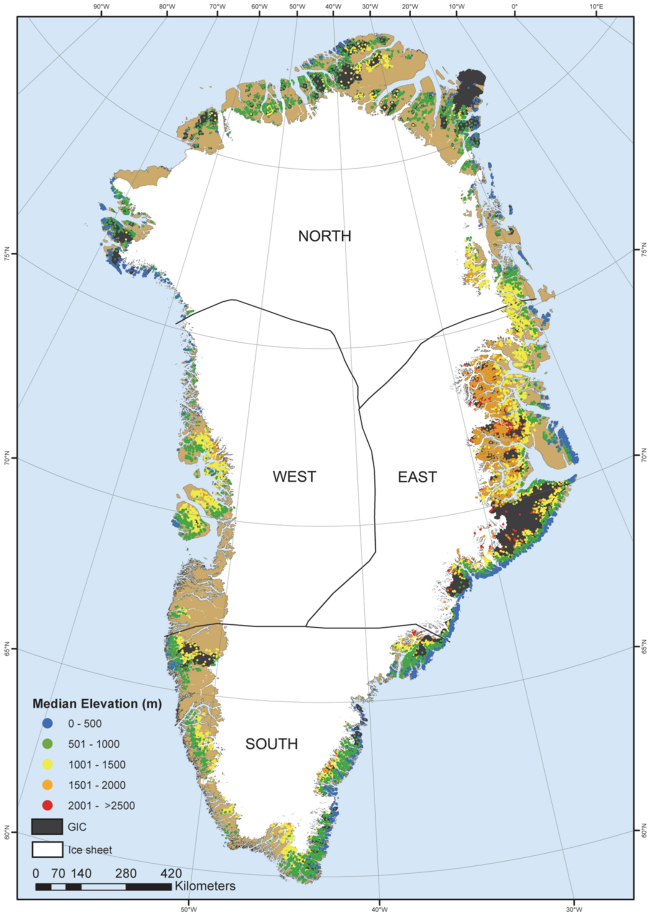

Fig. 8. Color-coded visualization of median elevation for all GIC. Local GIC are shown in dark grey in the background.

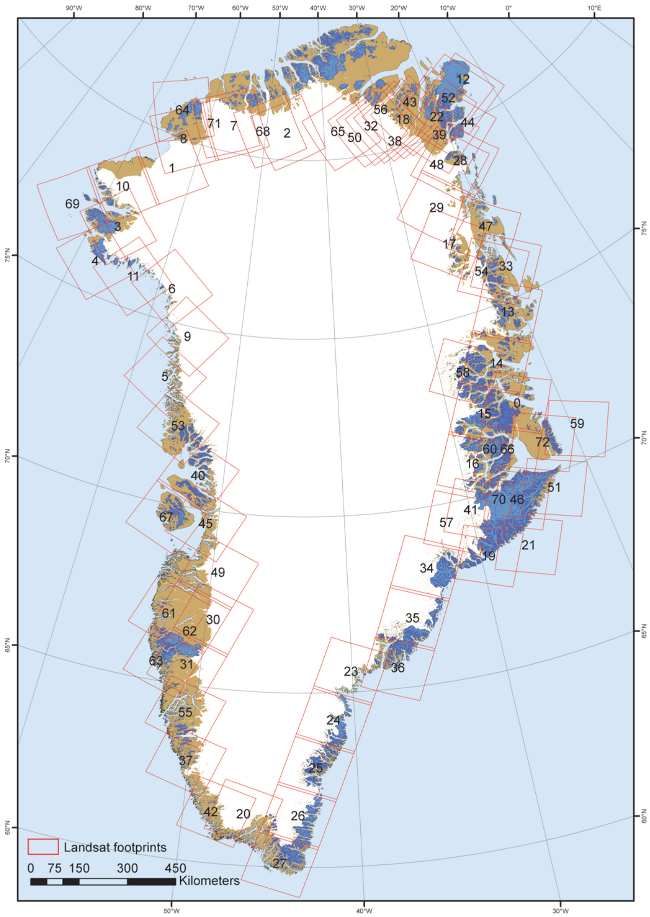

Fig. A1. Scene location (footprint) overview map (see Table A1 for path, row and acquisition date). Local GIC are shown in blue in the background.

Fig. A2. Location map of all marine terminating glaciers in Greenland with glacier areas in dark grey.